A STUDY INTO HAMMER MILL ROTOR AND HAMMER CONSTRUCTION AND SHOCK EQUILIBRATION

Gh. Voicu[1], G. Moiceanu[1*], M. Chițoiu[1], G. Paraschiv[1], D.C. Carp-Ciocârdia[1]
[1] University Politehnica of Bucharest, Bucharest, ROMANIA, [*]moiceanugeorgiana@gmail.com

Abstract (TNR 9 pt Bold): *Hammer mill grinding process must be researched from two points of view: design and costruction of hammer mills and studying the working process using different material subjected to grinding. This paper analyses MC22 hammer mill hammers and rotor construction by evaluating their shock equilibration and the rotor static equilibration. Hammer constructive parameters which have a significant influence over mill performance was studied. Choosing the right parameters assures a low vibration workflow which implies a rise in hammer mill lifespan. This optimum set-up is achieved through adopting certain shock equilibration conditions for hammers and rotor.*

Keywords (TNR 9 pt Bold): *hammer mill, shock equilibration, working elements, inertia moment, hammer*

1. INTRODUCTION GH

An important problem in designing and construction of hammer mills used for biomass grinding is determining rotor and hammer constructive parameters. Constructive parameters of the two components have a significant influence over mill performance. Choosing the right parameters assures a low vibration workflow which contributes to a rise in exploitation period.

For an extension on the exploitation period, certain material feed conditions are adopted and a stable rotation movement is assured for hammers in the grinding process, and particle clashes with the hammers don't produce percussion in the bond joints, and the mill rotor is balanced both statically and dynamically, [2].

The design and construction of hammer mill are important in processing the material subjected to grinding. Hammer mill uses high-velocity rotating shafts to impart kinetic energy to the processed material. The biomass is heat by the hammers until it is small enough to pass through sieves. The hammers can be be inverted and rotated such that each hammer can be used in two or four different positions. Also, the hammers can be fixed or freely swinging, [4].

Studying the design of hammer in paper [5] the authors used as a baseline a commercial grinder. They attached to the mill two different hammer designs to the mill. Also, scientists changed the number of hammers and changed their speed by modifying the grinding drum and drive pulleys. After all design plans were done they used three different feedstocks corn stover, switchgrass and wheat straw for experimental tests. They concluded that modifying the hammers of a small-scale grinder resulted in increased capacity and efficiency. Changing the tip speed in this case also resulted in a net improvement over the original speed of the hammer mill by as much as 300%, [5].

2. MATERIAL AND METHODES. TEORETICAL ELEMENTS

Balance parameters analysis was done on MC-22 hammer mill which was studied for hammer shock equilibration. Hammer equilibration condition is achieved if the percussion that appears in joints to the rotor is null. According to specialty literature [1, 2], tangent component of this percussion is null when hammers perpendicularly hit the material. In order for this to be achieved, mill material feeding is usually achieved on a tangential path. Considering that percussions apply on hammer periphery, the normal component of percussion is equal to zero only if the *l* hammer length (fig. 1) satisfies the following relation:

$$l = \frac{J_{O_1}}{M \cdot c} \quad (1)$$

where: J_{O1} is the hammer mechanical inertia moment in relation to its articulation axis ($kg \cdot m^2$); M – hammer mass (kg); c – distance from the hammer articulation axis to its center mass (C_m).

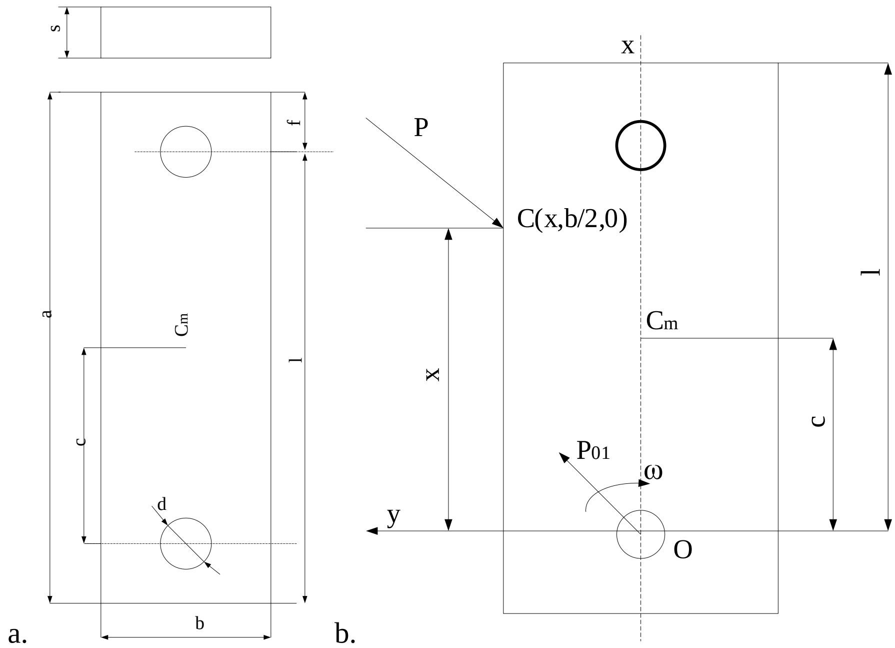

Figure 1: a. Normal hammer shape and dimensions. b. Calculus scheme for hammer shock equilibration [1]

In the case of a normal two-hole hammer, the inertia moment, in relation to the oscillation axis, is determined by the Steiner theorem, [1].

$$J_{01} = J_{cm} + (M - 2m_o)c^2 \quad (2)$$

$$J_{cm} = \frac{M}{12}(a^2 + b^2) - 2\left(\frac{m_o d^2}{8} + m_o c^2\right) \quad (3)$$

$$l = \frac{a^2 + b^2}{12c} - \frac{2m_o}{M\,c}\left(\frac{d^2}{8} + c^2\right) + \left(1 - \frac{2m_o}{m}\right)c \quad (4)$$

Where: m_o mass of the d diameter disc. So, considering that $m_o/M = 0$ then l becomes, [2]:

$$l = \frac{a^2 + b^2}{12c} + c \quad (5)$$

Position of the holes is given by f, which gives us the opportunity to think of hypotheses regarding hammer shock equilibration. a and b represent hammer length and width [1].

$$c = \frac{a}{2} - f \quad (6)$$

$$l = a - f \quad (7)$$

$$f = \frac{a}{3} - \frac{b^2}{6a} \quad (8)$$

For MC-22 hammer mill shock equilibration, four types of hammers of different edges, but identical general dimensions were used. These hammers are represented in figure 2, and their dimensions are shown in table 1.

Table 1: Dimensions of each hammer

	Hammer type A	Hammer type B	Hammer type C	Hammer type C		Hammer type A	Hammer type B	Hammer type C	Hammer type C
a	153	153	153	153	b_4	-	-	8.5	-
b	60	60	60	60	b_4'	-	-	4.5	-
d	21	21	21	21	b_5	-	-	5.66	-
b_1	8.5	-	-	-	b_5'	-	-	4.5	-
b_1'	9	-	-	-	b_6	-	-	2.83	-
b_2	-	8.5	-	-	b_6'	-	-	4.5	-
b_2'	-	4.5	-	-	b_7	-	-	-	8.5
b_3	-	5	-	-	b_7'	-	-	-	9
b_3'	-	4.5	-	-					

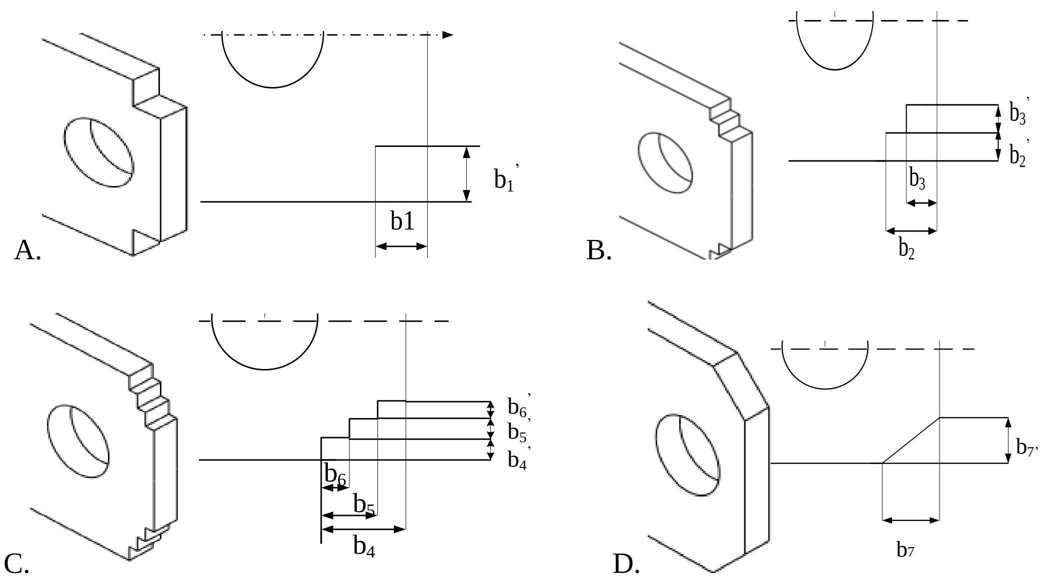

Figure 2: Types of hammers used for shock equilibration

So, it was started from the general case which implies that the mechanical inertia moment in relation to the hammer rotation axis is:

$$J_{01} = Jc_m + M \cdot c^2 \tag{8}$$

where; J_{Cm} is the hammer mechanical inertia moment in relation to its center mass.
Calculus equations were used for the four cases. Each time, the formed rectangle and triangle center was noted, so that the inertia moment and hammer mill for each case were able to be calculated. (CC_1 – distance from the hammer center to the rectangle center formed by the b_1 and b_1', on the direction of the longitudinal axis, similarly CC_2, CC_3, CC_4, CC_5, CC_6, CC_7,).

a) Type A hammer case – hammer with rectangle edge

$$(CC_1)^2 = \left(\frac{b}{2} - \frac{b_1'}{2}\right) + \left(\frac{a}{2} - \frac{b_1}{2}\right)^2 = \frac{1}{4}\left[(b - b_1')^2 + (a - b_1)^2\right] \tag{9}$$

$$Jc_A = \rho \cdot s \cdot \left[\frac{ab}{12}(a^2 + b^2) - \frac{\pi d^2}{2}\left(\frac{d^2}{8} + c^2\right) - 4\left[\frac{bb_1'}{12}(b_1^2 + b_1^{2'}) + bb_1'(CC_1)^2\right]\right] \tag{10}$$

$$M_A = \rho \cdot s \cdot \left[ab - \frac{2\pi d^2}{4} - 4bb_1'(CC_1)^2\right] \tag{11}$$

Knowing both inertia moment and hammer mass, with the help of relation (8), mechanical inertia moment in relation with hammer rotation axis is determined. The result contributes to c, l and f dimension determination. Type B hammer case – hammer with two rectangle steppes

$$(CC_2)^2 = \frac{1}{4}\left[(b - b_2^{'})^2 + (a - b_2)^2\right] \tag{12}$$

$$(CC_3)^2 = \left(\frac{b}{2} - b_2^{'} - \frac{b_3^{'}}{2}\right)^2 + \left(\frac{a}{2} - \frac{b_3}{2}\right)^2 \tag{13}$$

$$Jc_B = \rho \cdot s \cdot \left[\begin{array}{l} \frac{ab}{12}\left(a^2 + b^2\right) - \frac{\pi d^2}{2}\left(\frac{d^2}{8} + c^2\right) - 4\frac{b_2 b_2^{'}}{12}\left(b_2^2 + b_2^{'2}\right) - 4b_2 b_2^{'}(CC_2)^2 - \\ -4\frac{b_3 b_3^{'}}{12}\left(b_3^2 + b_3^{'2}\right) - 4b_3 b_3^{'}(CC_3)^2 \end{array}\right] \tag{14}$$

$$M_B = \rho \cdot s \cdot \left[ab - \frac{2\pi d^2}{4} - 4b_2 b_2^{'}(CC_2)^2 - 4b_3 b_3^{'}(CC_3)^2\right] \tag{15}$$

b) Type C hammer case – hammer with three rectangle steppes

$$(CC_4)^2 = \frac{1}{4}\left[(b - b_4^{'})^2 + (a - b_4)^2\right] \tag{16}$$

$$(CC_5)^2 = \left(\frac{b}{2} - b_4^{'} - \frac{b_5^{'}}{2}\right)^2 + \left(\frac{a}{2} - \frac{b_5}{2}\right)^2 \tag{17}$$

$$(CC_6)^2 = \left(\frac{b}{2} - b_4^{'} - b_5^{'} - \frac{b_6^{'}}{2}\right)^2 + \left(\frac{a}{2} - \frac{b_6}{2}\right)^2 \tag{19}$$

$$Jc_C = \rho \cdot s \cdot \left[\begin{array}{l} \frac{ab}{12}\left(a^2 + b^2\right) - \frac{\pi d^2}{2}\left(\frac{d^2}{8} + c^2\right) - 4\frac{b_4 b_4^{'}}{12}\left(b_4^2 + b_4^{'2}\right) - 4b_4 b_4^{'}(CC_4)^2 - 4\frac{b_5 b_5^{'}}{12}\left(b_5^2 + b_5^{'2}\right) \\ -4b_5 b_5^{'}(CC_5)^2 - 4\frac{b_6 b_6^{'}}{12}\left(b_6^2 + b_6^{'2}\right) - 4b_6 b_6^{'}(CC_6)^2 \end{array}\right] \tag{19}$$

$$M_C = \rho \cdot s \cdot \left[ab - \frac{2\pi d^2}{4} - 4b_4 b_4^{'}(CC_4)^2 - 4b_5 b_5^{'}(CC_5)^2 - 4b_6 b_6^{'}(CC_6)^2\right] \tag{20}$$

c) Type D hammer case – hammer with triangle shaped edges

$$(CC_7)^2 = \left(\frac{b}{2} - \frac{b_7^{'}}{3}\right)^2 + \left(\frac{a}{2} - \frac{b_7}{2}\right)^2 \tag{21}$$

$$Jc_D = \rho \cdot s \cdot \left[\frac{ab}{12}\left(a^2 + b^2\right) - \frac{\pi d^2}{2}\left(\frac{d^2}{8} + c^2\right) - 4\frac{b_7 b_7^{'}}{36}(b_7^2 + b_7^{'2}) - \frac{4b_7 b_7^{'}}{2}(CC_7)^2\right] \tag{22}$$

$$M_D = \rho \cdot s \cdot \left[ab - \frac{2\pi d^2}{4} - - \frac{4b_7 b_7^{'}}{2}(CC_7)^2\right] \tag{23}$$

where: ρ is hammer material density, s – hammer width.
Regarding rotor static and dynamic equilibration, we can say that these are given by the relations:

$$x_0 = 0, y_0 = 0, \tag{24}$$

Which is conditioned by an equal number of hammers, on opposed bolts (and an even number of bolts and joints).

$$J_{yz} = M \cdot \sum_{i=1}^{k} y_i \sum_{j=1}^{N_i} z_i = 0 \tag{25}$$

$$J_{zx} = M \cdot \sum_{i=1}^{k} x_i \sum_{j=1}^{N_j} z_i = 0 \tag{26}$$

where: N_i is the number of hammers on bolt i, k – number of hammer bolts, z_i – distance on Oz axis of hammer j, M – hammer mass, x_i, y_i – coordinates of the center mass of hammers on i bolt.

3. RESULTS AND DISCUSSION

Calculated data for each of the four hammer types from figure 2 are presented in tables 2 and 3. Each time, values of l, c, J_{O1}, M and f were calculated starting from the known values of a hammer length, b hammer width, the fix hole diameter and the edge dimensions for each type of hammer.

Table 2: Calculated values of hammer mills weight and moment of inertia (rotative moment)

Hammer type	Hammers weight M [kg]	Moment of inertia in the center of the hammer J_c	Moment of inertia J_{O1}
Full hammer	0,576	$1.29 \cdot 10^{-3}$	$3.19 \cdot 10^{-3}$
Hammer with fixation holes	0,533	$1.15 \cdot 10^{-3}$	$2.91 \cdot 10^{-3}$
A	0,53291	$1,65 \cdot 10^{-5}$	$1.77 \cdot 10^{-3}$
B	0,53293	$1,68 \cdot 10^{-5}$	$1.78 \cdot 10^{-3}$
C	0,53290	$1,65 \cdot 10^{-5}$	$1.78 \cdot 10^{-3}$
D	0,533	$1,73 \cdot 10^{-5}$	$1.78 \cdot 10^{-3}$

Table 3: Calculated values l, c and f

Hammer type	l	c	f calculated	f real
Full hammer	105,92	29.42	47.07	10
Straight edge hammer	103.94	30.75	45.75	10
A	107.39	30.91	45.57	10
B	107.39	30.91	45.57	10
C	107.39	30.91	45.57	10
D	107.39	30.91	45.57	10

We can see that there are significant differences between inertia moments J_c and J_{O1} (towards the hammer center mass and in relation to the rotor articulation point) according to the action edge geometrical form. It is fundamental that all the edges respect execution prescriptions, in order to avoid differences and shape errors that can lead to an irregular performance.
Regarding level f for the shock equilibration of hammer, calculated values are significantly different from the real value, which means that the producer did not respect theoretical specifications. This can lead to a vibration high performance and ultimately to a shortened mill lifespan. For hammer rotor static and dynamic equilibration check, the rotor hammer distribution graph was drawn (fig 3).

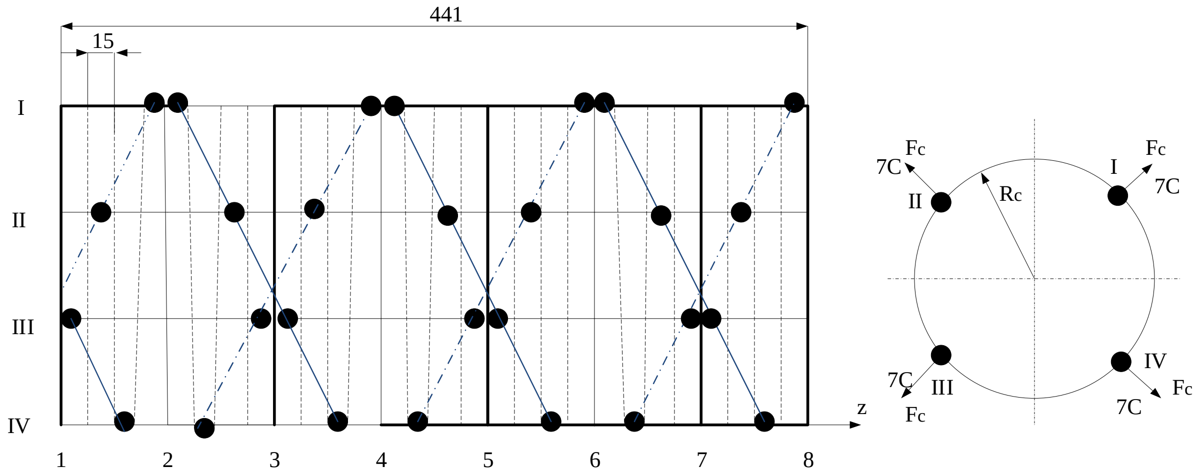

Figure 3: Hammer distribution scheme following helicoidal lines

A helicoidal line distribution for the hammers can be seen, which would lead to a better performance compared to other distribution methods. Relations of dynamic equilibration check are represented by relation (25) where J_{yz}=0 şi J_{zx}=0. Equilibration conditions for the position in figure 3 is:

$$J_{yz} = M \cdot \left[R_c \cdot \tfrac{\sqrt{2}}{2} \cdot \sum z_{Ii} + R_c \cdot \tfrac{\sqrt{2}}{2} \cdot \sum z_{IIi} - R_c \cdot \tfrac{\sqrt{2}}{2} \cdot \sum z_{IIIi} - R_c \cdot \tfrac{\sqrt{2}}{2} \cdot \sum z_{IVi} \right] = 0 \quad (27)$$

$$J_{xz} = M \cdot \left[R_c \cdot \tfrac{\sqrt{2}}{2} \cdot \sum z_{Ii} - R_c \cdot \tfrac{\sqrt{2}}{2} \cdot \sum z_{IIi} - R_c \cdot \tfrac{\sqrt{2}}{2} \cdot \sum z_{IIIi} + R_c \cdot \tfrac{\sqrt{2}}{2} \cdot \sum z_{IVi} \right] = 0 \quad (28)$$

Because $\sum z_{Ii} \neq \sum z_{IIi} \neq \sum z_{IIIi} \neq \sum z_{IVi}$ according to execution drawing, the moment of inertia value is different from zero, thus being $J_{yz}=1.45 \cdot 10^{-4}$ kg·m^2 and $J_{zx}=4.63 \cdot 10^{-4}$ kg·m^2.

4. CONCLUSION

Rotor hammer equilibration is very important for a good hammer mill function without vibrations. Our verification for a Romanian hammer mill MC 22 led to two major conclusions:

- Hammer are not shock equilibrated (there is a major difference between calculated f and real f from 47 mm to 10 mm);
- There is a small value for the moment of inertia, different from zero for execution mill drawing heights.

These differences can lead to mills shut down after a smaller number of usage hours than the one intended due to a vibration working process. Our experimental results can support the constructor in constructing optimization of MC-22 mill and for all hammer mills, in general.

REFERENCES

[1] Chelemen I., Maşini si instaşaţii zootehnice Partea II, Institutul Politehnic Bucureşti, 1983;

[2]Voicu G., Casandroiu T., David L., Parametrii constructive ai cicoanelor de la morile cu ciocane, nomograma de calcul, Constructia de masini, nr 8-9, Institutul Polithenic Bucuresti, 1990;

[3] Carte tehnica moara cu ciocane MC 22;

[4] Mohamed T.H, Radwan H.A., Elashhab A.O., Adly N.Y., Design and evaluate of a small hammer mill, Eqypt Journal Agricultural Res, No. 93 (5)(B), 2015;

[5] Yancey N., Wright C.T., Westover T., Optimizing hammer mill performance through screen selection and hammer design, Biofuels, pp. 85-94, 2014